Nanomed Res J 9(1):61-70, Winter 2024

RESEARCH ARTICLE

Preparation of silver-containing starch nanocomposite prepared from green synthesis with green tea plant extract and investigation of dye degradation and antibacterial activity

Ehsan Beigi Baktash[1], Negar Motakef Kazemi[2,*], Sepideh Hamedi[3]

[1] Department of Nanochemistry, Faculty of Pharmaceutical Chemistry, Tehran Medical Sciences, Islamic Azad University, Tehran, Iran.

[2] Department of Medical Nanotechnology, Faculty of Advanced Sciences and Technology, Tehran Medical Sciences, Islamic Azad University, Tehran, Iran.

[3] Faculty of New Technologies Engineering, Shahid Beheshti University, Zirab Campus, Mazandaran, Iran.

ARTICLE INFO

Article History:
Received 16 Jan 2024
Accepted 23 Mar 2024
Published 01 Apr 2024

Keywords:
Antibacterial activity
Degradation
Green synthesis
MB
Ag NPs
Starch

ABSTRACT

Objective(s): In this work, silver nanoparticles (Ag NPs) were synthesized by green tea plant extract as an easy, cost-effective, environmentally friendly, and reliable synthesis. The silver nanocomposite with different amounts of starch (0.5, 1, 1.5 g) were prepared. Then, the methylene blue (MB) dye degradation and the antibacterial activity of the nanocomposite were evaluated as an environmental challenge.

Methods: The samples were characterized using scanning electron microscope (SEM) for observation size and morphology, energy dispersive X-ray analysis (EDX) for determination elemental analysis, Fourier transform infrared spectroscopy (FTIR) for investigation functional groups, and X-ray diffraction analysis (XRD) for confirmation crystalline structure. The catalytic properties of the synthesized samples were studied in MB degradation.

Results: The maximum degradation (more than 90%) was related to Ag NP with 0.5 g of starch. The antibacterial activity of Ag NPs and nanocomposites was investigated against *Staphylococcus aureus (S. aureus)* as *Gram-positive* and *Pseudomonas aeruginosa (P. aeruginosa)* as Gram-negative bacteria. The samples indicated inhibitory activity with suitable inhibition zone and were more effective against *S. aureus* as compared to *P. aeruginosa.*

Conclusions: In general, the green synthesis of Ag NP-starch has good catalytic potential in MB degradation in an aqueous medium in a short time with high efficiency.

How to cite this article
Beigi Baktash E., Motakef Kazemi N., Hamedi S. Preparation of silver-containing starch nanocomposite prepared from green synthesis with green tea plant extract and investigation of dye degradation and antibacterial activity. Nanomed Res J, 2024; 9(1): 61-70. DOI: 10.22034/nmrj.2024.01.007

INTRODUCTION

The main problem threatening the environment is water pollution. The organic and inorganic dyes as major contaminants can enter water sources as sewages [1]. Many industries such as leather, textile, plastic, paper, medicine, cosmetics, and food are the sources of organic dye released to aqueous environment. Carcinogenicity and mutagenicity is one of the disadvantages of these dyes [2]. One of the cationic phenothiazine dyed is MB, which is widely used in coloring paper, wools, dyeing cotton, etc. Its harmful effects on humans with a higher concentration of 2 ppm led to eye and skin irritation, headache, nausea, diarrhea, vomiting, and respiratory problems [3,4]. The presence of MB in the dye and textile industries effluents is due to the high solubility of MB in water. Therefore, it is very important to remove, reduce, destroy and decolorize this dye from water systems [5]. Several

* Corresponding Author Email: *motakef@iaups.ac.ir*

techniques such as biodegradation [6,7], advanced oxidation [8], ultrafiltration [9], ozonation [10], electrocoagulation [11], etc. have been reported to remove MB from aqueous solutions. Catalytic degradation of dyes using metal nanoparticles has attracted much attention due to their remarkable catalytic activities and effective removal of dyes [12]. These materials have high surface and selectivity, antimicrobial and photocatalytic activity, as well as low energy cost, which are suitable options for the treatment of water from dyes [13].

One of the examples of these metal NPs that have been used to remove different dyes are Ag NPs. Ag NPs have received much attention due to their high conductivity and stability, excellent adsorption capacity, high surface area, good catalytic activity, and antibacterial and antiviral properties [14,15]. Generally, Ag NPs are synthesized using physicochemical methods such as laser ablation [16], photochemical reduction [17], electrochemical techniques [18], gamma irradiation [19], microwave [20], and chemical reduction [21]. The mentioned approaches have high efficiency, but have limitations such as high functional cost, use of toxic chemicals, and high energy requirements. To overcome these drawbacks, green synthesis of Ag NPs has been reported as a cost-effective and eco-friendly method using plant extracts, microorganisms and natural polymers [22]. The most prominent problem related to Ag NPs is that they tend to agglomerate, duo to their high surface energy, which can negatively affect their chemical stability and catalytic properties [23]. To overcome these limitations, support materials such as graphene [24], graphene oxide [25], activated carbon [26], silica [27], etc. can be used.

Natural polysaccharides have been able to attract a lot of attention for wastewater treatment duo to their environmentally friendly, low-cost, abundance, and biodegradability nature [28]. Starch is one of the polysaccharides as a natural polymer, which can be used as an ideal support. Its characteristics include low-cost, non-toxicity, high abundance, high surface area, biocompatibility, and renewable [29,30]. In this study, Ag NPs were synthesized at room temperature and 90 °C by the green tea plant extract. Also, silver nanocomposite with different percent of starch were prepared. Nanoscale size by SEM, compound elements by EDX, functional groups and compound qualitative preparation by FTIR, and crystal structure by XRD were investigated. The catalytic activity of samples was evaluated for MB dye degradation in an aqueous solution. The antibacterial effect of samples against *S. aureus* and *P. aeruginosa* bacteria was presented by examining average halo diameter, minimum inhibitory concentration (MIC) and minimum bactericidal concentration (MBC).

MATERIALS AND METHODS

Materials

Silver nitrate ($AgNO_3$) 99%, MB 99%, and glycerol were purchased from Merck. Potato starch was prepared from Tetra-Chem. *S. aureus* strain (ATCC 6538) and *P. aeruginosa* strain (ATCC15442) were procured from Kit-Iran. Antibiogram disk was prepared from Padtan Teb. Mueller–Hinton agar growth medium was purchased from Merck.

Methods

Preparation of green tea extract

The green tea plant was cleaned and washed. After drying in the shade, it was ground. 20 g of green tea plant powder with 100 mL of deionized water in an Erlenmeyer flask was heated for 70 min in a water bath to obtain the primary plant extract. The aqueous extract was filtered using Whatman No. 1 filter paper and a syringe filter. Then, it was kept in a Falcon tube in dark glass at room temperature.

Preparation of Ag NPs

10 mL of 0.001 M $AgNO_3$ solution was mixed with 90 mL of green tea extract. The resulting solution was separately stirred at a temperature of 25 and 90 °C. In order to reduce silver ions, the solution was kept at room temperature in a dark place overnight. The color change of the extract from pale yellow to dark brown to black indicates the production of Ag NPs. The solution was centrifuged at 10,000 rpm for 10 min to separate the NPs from the solvent. The nanomaterials were washed with deionized water and placed in an electric furnace (KSL-1700X-A4) at 450 °C. The obtained Ag NPs were stored inside the microtube at 4 °C.

Preparation of nanocomposite

Ag NPs solutions with a concentration of 0.01 M were prepared using deionized water as solvent. For this purpose, NPs prepared at 90 °C were used, because these NPs were in better condition in terms of morphological properties. Using potato

starch with the amounts of 0.5, 1, and 1.5 g, as well as a mixture of deionized water and glycerol with a ratio of 85:15, solutions were prepared and used to prepare Ag NPs. To make uniform these samples, all starch solutions were stirred at 40 °C for 1 h in the paraffin bath. In the next step to prepare nanocomposites, 1 mL of solutions prepared from Ag NPs was added separately to potato starch solutions to provide three nanocomposites based on the amount of potato starch.

Investigation of dye degradation

MB solution was prepared with an initial concentration of 0.0001 M and stirred for 1 h. $NaBH_4$ solution (0.05 M) was added to 10 mL of MB solution (10 M) under vigorous stirring for 5 min. Then, 2 mL of NPs solution was added and stirred for 5 min. MB is blue in the oxidation medium and then decolorizes in the presence of the reducing agent ($NaBH_4$), indicating the reduction of MB to leucomethylene blue. The progress of the reaction was monitored using a UV-Vis spectrophotometer at regular intervals.

Investigation of antibacterial activity

Two gram-positive bacteria and gram-negative bacteria named *S. aureus* and *P. aeruginosa* have been used. In order to evaluate the antimicrobial properties of Ag NPs, an antimicrobial susceptibility test was selected and agar well diffusion was utilized. In this method, the growth inhibition halo was entered into a surface of the agar medium in the plates through an external antibiotic diffusion from a source (holes created in the agar layer). The halo size of the growth inhibition zone around each hole indicates antimicrobial activity, which is the most common form of antimicrobial evaluation and is known as the Kirby-Bauer test. The basis of this method is the transfer of antibacterial material into the disk. First, sterile disks were placed in the extract solution and after soaking, they were used. 5 mm thick Muller Hinton agar medium was added to selected sterile Petri dishes. The bacterial sample was removed from the base growth medium by the applicator and inoculated into the growth medium. Finally, the inoculated Petri dishes were placed in the incubator at 37 °C. After 24 h, the diameter of the growth inhibition halos created around the disc was measured with a caliper.

MIC and MBC tests were performed by a Microdilution method. In this method, using 96-well microplates, different concentrations of Ag NPs and silver nanocomposites (0.39, 0.78, 1.56, 3.125, 6.25, 12.5, 25, 50, 100 μg ml^{-1}) were studied against *P. aeruginosa* and *S. aureus*, as well as the growth of bacteria versus synthesized NPs and nanocomposites was evaluated. First, an equal amount of 95 μL of Mueller-Hinton broth was poured into 96 microplates well. To the first tube was added 100 μL of NPs with a concentration of 100 μg per μL, which after mixing, the dilution of the desired NPs in the first tube was reduced by half. Then, 100 μL were taken from the first tube and added to the second tube, dilution was performed until the last tube, where the dilution of NPs in each tube was half of the previous tube. The last well contained 195 μL of Mueller-Hinton broth and 5 μL of microbial suspension but no test compound, which was considered a negative control. Then, all wells except well 12 were inoculated with 5 μL of bacterial suspension (1.5×10^8 CFU/mL). After closing the lid, the Microplates were incubated for 24 h at 37 °C. The turbidity of the wells was then visually read and the growth or non-growth of bacteria was examined. The lowest concentration of NPs in which no bacteria survived was considered as MBC.

Characterization

SEM TESCAN model MIRA lll made by the Czech Republic company to evaluate the morphology and size. FTIR of Thermo device Avatar model made in USA by KBr tablets at room temperature to check the functional group. XRD device of Philips model PW1730 made in the Netherlands to determine the crystal structure. BET device of Bel model BELSORP MINI ll made in Japan to measure the surface area. UV-Vis spectrophotometer PG Instrument model T80 made in Australia to study the amount of MB absorption,

RESULTS AND DISCUSSION

SEM

SEM images of Ag NPs at room temperature and 90 °C, as well as Ag NPs with starch, are shown in Fig 1 a and b. Based on the results, the surface of the silver + starch nanocomposite has a uniform structure with many cracks, which can be due to the synthesis process (Fig. 1c). Based on the results, applying a temperature of 90 °C (instead of ambient temperature) resulted in the formation of uniform nanoparticles with a narrow size distribution. Therefore, nanoparticles prepared at a temperature

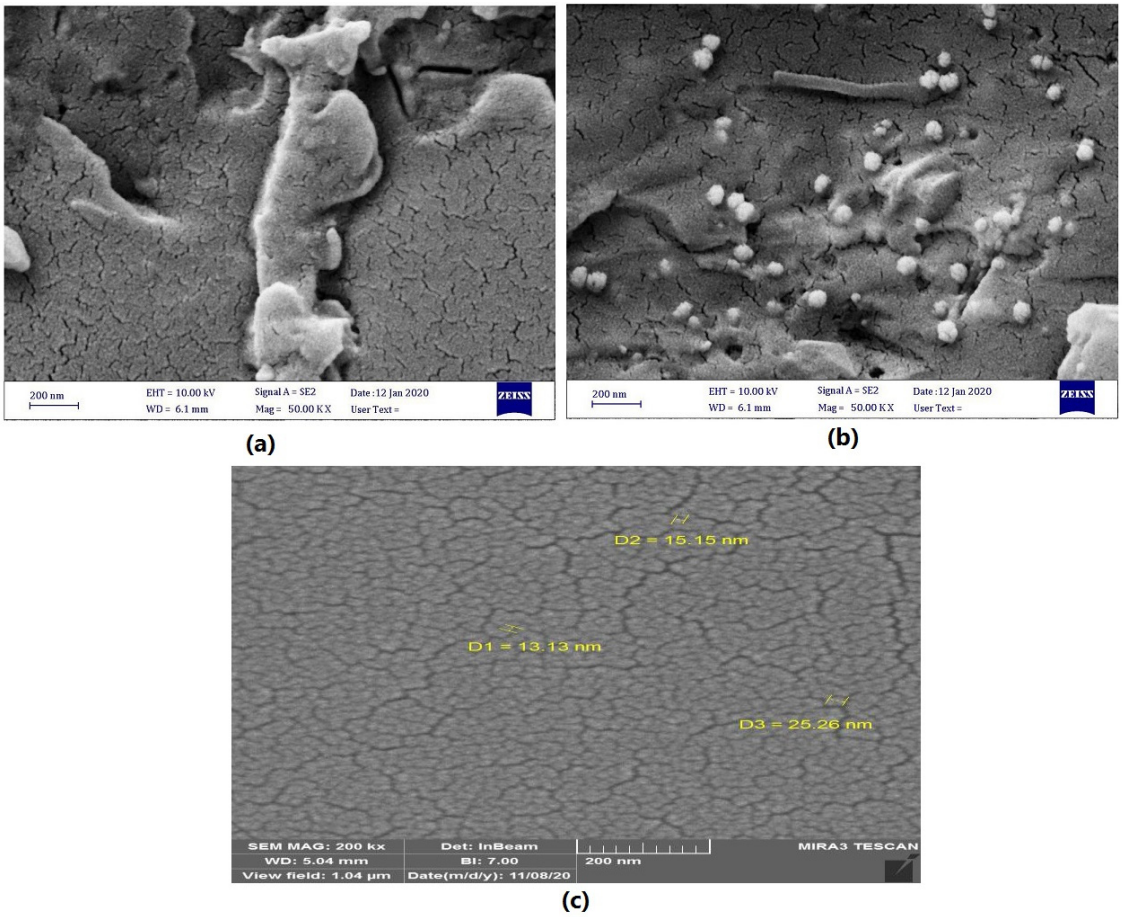

Fig 1. SEM images of Ag NPs at (a) room temperature, (b) 90 °C, and (c) Ag NPs + starch nanocomposite.

of 90 °C were used to prepare the nanocomposite.

EDX

The EDX spectra (Fig 2) indicate the confirmation of the formation of Ag NPs at room temperature and 90 °C. At room temperature, the weight percentage of C, Ag, and O was 69.4%, 3.8%, and 26.8%, respectively. On the other hand, the values of 48.7%, 29.5%, and 21.9% were obtained for C, Ag, and O at 90 °C, respectively. The elements of C and O were also found, which reveal the presence of plant phytochemicals as capping elements on the NPs surface [31]. The purity of prepared Ag NPs was confirmed via the absence of other elements.

FTIR

FTIR spectra of synthesized Ag NPs with two different temperatures are presented in Fig 3. The strong and wide peaks at 3417 and 3420 cm^{-1} indicate the presence of phenolic compounds. Also, this is attributed to the O-H stretching vibration. The absorption peaks at 2926 and 2927 cm^{-1} are assigned to the C-H stretching aromatic compound [32]. The absorption bands at 2362 and 2369 cm^{-1} demonstrate the presence of symmetric stretching of COO^- [33]. The stretching vibrations around 1690 and 1630 cm^{-1} are related to the C=O and N–H stretching of amide and amine bonds [34]. The observed absorption peaks at 1029 cm^{-1} are ascribed to C-O-C [35]. The bands around 874, 820, and 750 cm^{-1} are corresponding to the C–H, =C–H, and N–H [36].

Fig 3 displays the FTIR spectrum of nanocomposite containing Ag NPs and starch. A broad band at 3387 cm^{-1} attributed to the stretching of the hydroxyl group. The band at 2889 cm^{-1} is related to the asymmetric stretching of C–H [37]. The peak at 1596 cm^{-1} represents C=O stretching (carbonyl group) [38]. The absorption peak at 1042 cm^{-1} is due to the C-O stretching of the

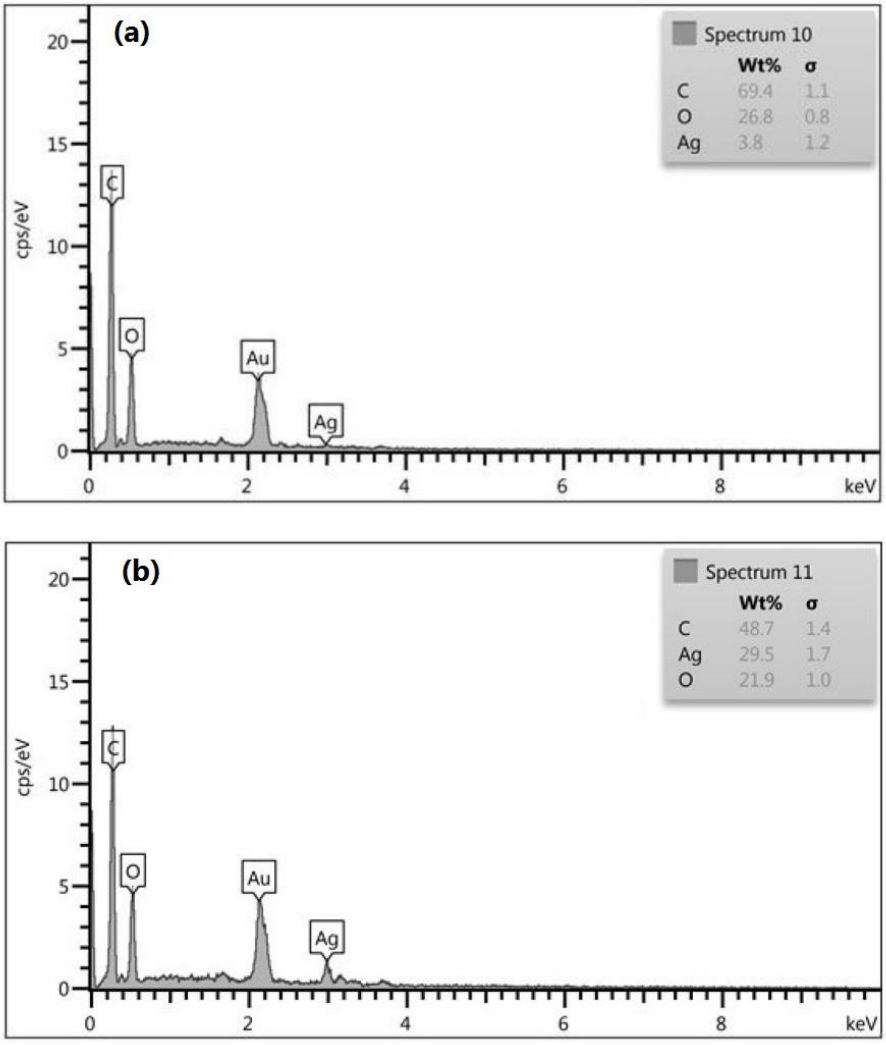

Fig 2. EDX pattern of Ag NPs at (a) room temperature and (b) 90 °C.

anhydroglucose rings [39].

XRD

The XRD pattern of Ag NPs with starch is displayed in Fig 4. The peaks appeared at 2θ = 38.15◦, 44.27◦, 64.49◦, and 77.39◦ which showed reflection at (111), (200) (220), and (311) in the region from 5 to 80◦ [40]. These results revealed the presence of Ag NPs (JCPDS No. 04-0783) with a face-centered cubic phase [37].

Dye degradation

In order to investigate the photocatalytic ability of synthesized materials with different amounts of starch in dye degradation, the initial dye concentration was considered to be 0.001 mg L^{-1} and the amount of degradation efficiency was obtained from Eq (1).

$$Degradation(\%) = \left(\frac{C_0 - C_t}{C_0}\right) \times 100 \quad (1)$$

Where C_t and C_0 show dye concentration at time t (mg L^{-1}) and initial concentration, respectively [41]. Fig 5 indicates that the maximum degradation efficiency (90%) value is assigned to the Ag Nps with 0.5 g starch in 65 min.

Antibacterial

The results of antibacterial tests for different samples are given in Table 1. According to the results, it can be seen that the lowest antibacterial

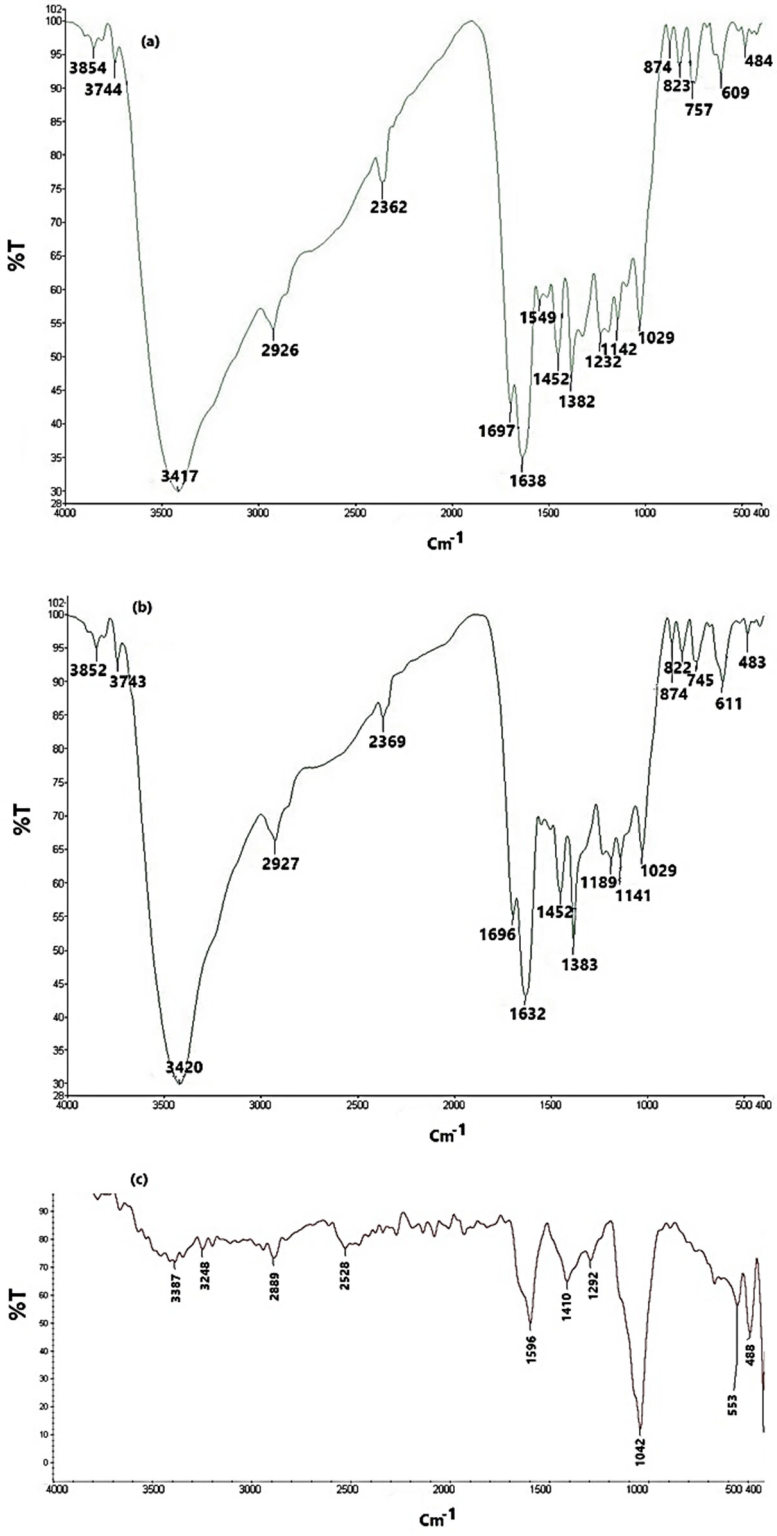

Fig 3. FTIR spectra of Ag NPs at (a) room temperature, (b) 90 °C, and Ag NPs + starch nanocomposite.

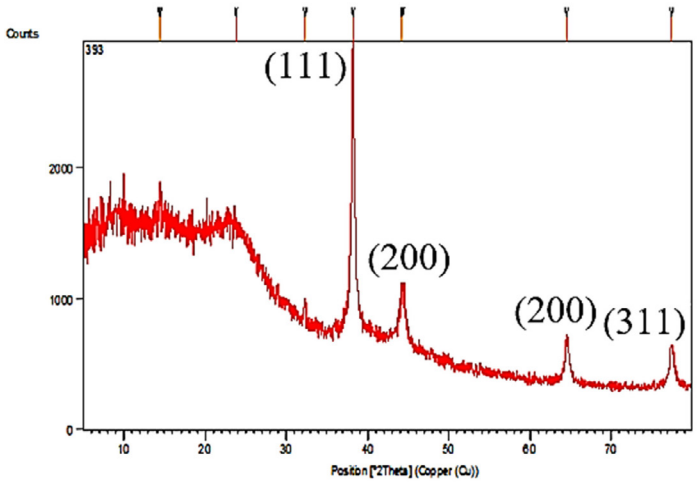

Fig. 4. XRD pattern of Ag NPs + starch nanocomposite.

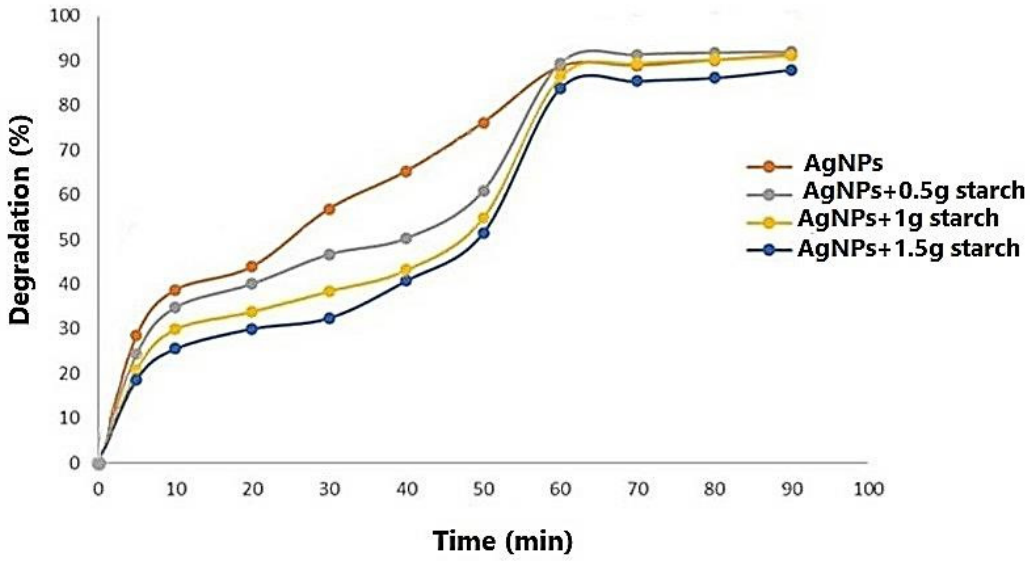

Fig 5. The degradation efficiency of Ag NPs and Ag NPs with different ratios of starch.

Table 1. Antibacterial test results based on average halo diameter.

Bacteria	*S. aureus*				*P. aeruginosa*			
	Ag NPs	Ag NPs + 0.5 g starch	Ag NPs + 1 g starch	Ag NPs +1.5 g starch	Ag NPs	Ag NPs + 0.5 g starch	Ag NPs + 1 g starch	Ag NPs + 1.5 g starch
Halo diameter (mm)	4.5	5	5.5	7	3.5	4.5	5	5

properties are related to *Pseudomonas* bacteria, which belongs to Ag NPs without starch. In addition, with increasing the concentration of starch, the antibacterial efficiency of Ag NPs improved and increased in the presence of the desired bacteria. The antimicrobial agent of silver is the presence of silver ions. Due to the high surface area of Ag NPs, they represent a strong and the acceptable bactericidal effect. The major reason for bactericidal features of Ag NPs is interfering with the totality of the bacterial cell by binding to necessary cellular structures, especially to

Table 2. Calculated MIC and MBC of Ag NPs and nanocomposites related to the *S. aureus* and *P. aeruginosa*.

Sample	*S. aureus*		*P. aeruginosa*	
	MIC (μg mL^{-1})	MBC (μg mL^{-1})	MIC (μg mL^{-1})	MBC (μg mL^{-1})
Ag NPs	12.5	25	25	50
Ag NPs+0.5 g starch	6.25	12.5	12.5	25
Ag NPs+1 g starch	3.12	6.25	12.5	25
Ag NPs+1.5 g starch	0.78	1.56	3.12	6.25

their SH-groups. Furthermore, Ag NPs produce reactive oxygen species (ROS) and free radicals, which destroy the bacterial cell wall and inhibit the respiratory enzymes. Finally, DNA replication can be disrupted by Ag NPs [42].

The results of MIC and MBC for *S. aureus* and *P. aeruginosa* are given in Table 2. The minimum concentration of samples that prevented the growth of bacteria was related to *S. aureus* and Ag NPs with 1.5 g of starch. Also, *S. aureus* as Gram-positive bacteria is more sensitive than *P. aeruginosa*. The highest concentration of MBC is related to Ag NPs without starch against *P. aeruginosa* and is equal to 50 μg mL^{-1}. The lowest concentration of MBC is assigned to Ag NPs with 1.5 g starch against *S. aureus*, which is equal to 1.56 μg mL^{-1}.

CONCLUSION

In the present study, the green tea plant extract was used as a reducing agent for the green synthesis of AuNPs at two different temperatures. Also, various amounts of starch along with Ag NPs were considered to prepare nanocomposite. The Ag NPs and nanocomposite were characterized using SEM, EDX, FTIR, and XRD methods. The photocatalytic ability of the synthesized Ag NPs and Ag NPs + starch nanocomposite was assessed using the degradation reaction of MB. The samples revealed outstanding catalytic activity in the dye degradation reaction. This simple, rapid, low-cost, eco-friendly, and green route can be utilized to treat aqueous media from toxic dyes. The Ag NPs alone and Ag NPs coupled with starch exhibited effective results against pathogenic strains, including *S. aureus* and *P. aeruginosa*. The samples depicted a zone of inhibition versus the mentioned gram-positive and Gram-negative bacteria. To summarize, this study presented a highly efficient nanocomposite of Ag NPs@starch as a potential candidate for the degradation of diverse dyes in industrial effluents.

CONFLICT OF INTEREST

The authors declare no conflict of interest.

REFERENCES

[1] Marimuthu S, Jayanthi Antonisamy A, Malayandi S, Rajendran K, Tsai PC, Pugazhendhi A, Kumar Ponnusamy V. Silver nanoparticles in dye effluent treatment: A review on synthesis, treatment methods, mechanisms, photocatalytic degradation, toxic effects and mitigation of toxicity, Journal of Photochemistry and Photobiology B: Biology. 2020;205:111823.

[2] Joseph S, Mathew B. Facile synthesis of silver nanoparticles and their application in dye degradation, Materials Science and Engineering B. 2015;195:90–97.

[3] Akkini Devi T, Ananthi N, Peter Amaladhas T. Photobiological synthesis of noble metal nanoparticles using Hydrocotyle asiatica and application as catalyst for the photodegradation of cationic dyes, Journal of Nanostructure in Chemistry. 2016;6:75-92.

[4] Singh J, Dhaliwal AS. Effective removal of methylene blue dye using silver nanoparticles containing grafted polymer of guar gum/acrylic acid as novel adsorbent, Journal of Polymers and the Environment. 2021;29:71-88.

[5] Rajasekar R, Samuel M, Jebakumar Immanuel Edison TN, Raman N. Sustainable synthesis of silver nanoparticles using Alstonia scholaris for enhanced catalytic degradation of methylene blue, Journal of Molecular Structure. 2021;1246:131208.

[6] Bharti V, Vikrant K, Goswami M, Tiwari H, Kumar Sonwani R, Lee J, Tsang DCW, Kim KH, Saeed M, Kumar S, Nath Rai B, Shekher Giri B, Sharan Singh R. Biodegradation of methylene blue dye in a batch and continuous mode using biochar as packing media, Environmental Research. 2019;171:356-364.

[7] Contreras M, David Grande-Tovar C, Vallejo W, Chaves-López C. Bio-removal of methylene blue from aqueous solution by galactomyces geotrichum KL20A, Water. 2019;11:282.

[8] Masoumbeigi H, Rezaee A. Removal of methylene blue (MB) dye from synthetic wastewater using UV/H_2O_2 advanced oxidation process, Journal of Health Policy and Sustainable Health. 2015;2:160-166.

[9] Arshad Khosa M, Sakhawat Shah S, Faizan Nazar M. Application of micellar enhanced ultrafiltration for the removal of methylene blue from aqueous solution, Journal of Dispersion Science and Technology. 2011;32:260–264.

[10] Nashmi OA, Abdulrazzaq NN, Mohammed AA. Removal of methylene blue from aqueous solution by ozone microbubbles, Association of Arab Universities Journal of Engineering Sciences. 2020;27:31-40.

[11] Mahmoud MS, Farah JY, Farrag TE. Enhanced removal of methylene blue by electrocoagulation using iron electrodes, Egyptian Journal of Petroleum. 2013;22:211-216.

[12] Qi L, Zhang K, Qin W, Hu Y. Highly efficient flow-through catalytic reduction of methylene blue using silver

nanoparticles functionalized cotton, Chemical Engineering Journal. 2020;388:124252.
[13] Atta AM, Moustafa YM, Al-Lohedan HA, Ezzat AO, Hashem AI. Methylene blue catalytic degradation using silver and magnetite nanoparticles functionalized with a poly (ionic liquid) based on quaternized dialkylethanolamine with 2-acrylamido-2-methylpropane sulfonate-co-vinylpyrrolidone, ACS Omega. 2020;5:2829-2842.
[14] Esmaili N, Mohammadi P, Abbaszadeh M, Sheibani H. Green synthesis of silver nanoparticles using Eucalyptus comadulensis leaves extract and its immobilization on magnetic nanocomposite (GO-Fe_3O_4/PAA/Ag) as a recoverable catalyst for degradation of organic dyes in water, Applied Organometallic Chemistry. 2020;34:e5547.
[15] Al-Senani GM, Al-Kadhi N. The synthesis and effect of silver nanoparticles on the adsorption of Cu^{2+} from aqueous solutions, Applied Sciences. 2020;10:4840.
[16] OhadiFar P, Shahidi Sh, Dorranian D. Synthesis of silver nanoparticles and exhaustion on cotton Fabric simultaneously using laser ablation method, Journal of Natural Fibers. 2020;17:1295-1306.
[17] Jara N, Milán NS, Rahman A, Mouheb L, Boffito DC, Jeffryes C, Amar Dahoumane S. Photochemical synthesis of gold and silver nanoparticles-A review, Molecules. 2021;26:4585.
[18] Khaydarov RA, Khaydarov RR, Gapurova O, Estrin Y, Scheper T. Electrochemical method for the synthesis of silver nanoparticles, Journal of Nanoparticle Research. 2009;11:1193-1200.
[19] He L, Dumee LF, Liu D, Velleman L, She F, Banos C, Davies JB, Kong L. Silver nanoparticles prepared by gamma irradiation across metal–organic framework templates, RSC Advances. 2015;5:10707-10715.
[20] Seku K, Reddy Gangapuram B, Pejjai B, Kumar Kadimpati K, Golla N. Microwave-assisted synthesis of silver nanoparticles and their application in catalytic, antibacterial and antioxidant activities, Journal of Nanostructure in Chemistry. 2018;8:179-188.
[21] Halder S, Ahmed AN, Gafur A, Seong G, Hossain MZ. Size-controlled facile synthesis of silver nanoparticles by chemical reduction method and analysis of their antibacterial performance, ChemistrySelect. 2021;6:9714-9720.
[22] Tarannum N, Divya, Gautam YK. Facile green synthesis and applications of silver nanoparticles: a state-of-the-art review, RSC Advances. 2019;9:34926-34948.
[23] Gupta S, Uhlmann P, Agrawal M, Chapuis S, Oertel U, Stamm M. Immobilization of silver nanoparticles on responsive polymer brushes, Macromolecules. 2008;41:2874-2879.
[24] Poornima Parvathi V, Parimaladevi R, Vasanth S, Umadevi M. Graphene boosted silver nanoparticles as surface enhanced raman spectroscopic sensors and photocatalysts for removal of standard and industrial dye contaminants, Sensors and Actuators B: Chemical. 2019;281:679-688.
[25] Rohaizad A, Shahabuddin S, Mehmood Shahid M, Maisarah Rashid N, Adlan Mohd Hir Z, Mukhlis Ramly M, Awang K, Wee Sionga C, Aspanut Z. Green synthesis of silver nanoparticles from Catharanthus roseus dried bark extract deposited on graphene oxide for effective adsorption of methylene blue dye, Journal of Environmental Chemical Engineering. 2020;8:103955.
[26] AbdEl-Salam AH, Ewais HA, Basaleh AS. Silver nanoparticles immobilised on the activated carbon as efficient adsorbent for removal of crystal violet dye from aqueous solutions. A kinetic study, Journal of Molecular Liquids. 2017;248:833-841.
[27] Das SK, Khan MR, Paranthamon T, Laffir F, Guha AK, Sekaran G, Baran Mandal A. Nano-silica fabricated with silver nanoparticles: Antifouling adsorbent for efficient dye removal, Effective water disinfection and biofouling control, Nanoscale. 2013;5:5549-5560.
[28] Radwan EK, El-Naggar ME, Abdel-Karim A, Wassel AR. Multifunctional 3D cationic starch/nanofibrillated cellulose/silver nanoparticles nanocomposite cryogel: Synthesis, adsorption, and antibacterial characteristics, International Journal of Biological Macromolecules. 2021;189:420-431.
[29] Nasrollahzadeh M, Sajjadi M, Iravani S, Varma RS. Starch, cellulose, pectin, gum, alginate, chitin and chitosan derived (nano) materials for sustainable water treatment: A review, Carbohydrate Polymers. 2021;251:116986.
[30] Li Y, Wang H, Xie J, Hou J, Song X, Dionysiou DD. Bi_2WO6-TiO_2/starch composite films with Ag nanoparticle irradiated by γ-ray used for the visible light photocatalytic degradation of ethylene, Chemical Engineering Journal. 2021;421:129986.
[31] Riaz M, Ismail M, Ahmad B, Zahid N, Jabbour G, Shafiq Khan M, Mutreja V, Sareen S, Rafiq A, Faheem M, Musaddiq Shah M, Khan MI, Imran Bukhari SA, Park J. Characterizations and analysis of the antioxidant, antimicrobial, and dye reduction ability of green synthesized silver nanoparticles, Green Processing and Synthesis. 2020;9:693-705.
[32] Al-Zaban MI, Mahmoud MA, AlHarbi MA. Catalytic degradation of methylene blue using silver nanoparticles synthesized by honey, Saudi Journal of Biological Sciences. 2021;28:2007-2013.
[33] Pirtarighat S, Ghannadnia M, Baghshahi S. Green synthesis of silver nanoparticles using the plant extract of Salvia spinosa grown in vitro and their antibacterial activity assessment, Journal of Nanostructure in Chemistry. 2019;9:1–9.
[34] Chouhan S, Guleria S. Green synthesis of AgNPs using Cannabis sativa leaf extract: Characterization, antibacterial, anti-yeast and a-amylase inhibitory activity, Materials Science for Energy Technologies. 2020;3:536–544.
[35] Grace Femi-Adepoju A, Oluwasogo Dada A, Opeyemi Otun K, Olufemi Adepoju A, Paul Fatoba O. Green synthesis of silver nanoparticles using terrestrial fern (Gleichenia Pectinata (Willd.) C. Presl.): characterization and antimicrobial studies, Heliyon. 2019;5:e01543.
[36] Rodríguez-Felix F, Guadalupe Lopez-Cota A, Jesús Moreno-Vasquez M, Zoraida Graciano-Verdugo A, Emedith Quintero-Reyes I, Lizette Del-Toro-Sanchez C, Agustín Tapia-Hernandez J. Sustainable-green synthesis of silver nanoparticles using safflower (Carthamus tinctorius L.) waste extract and its antibacterial activity, Heliyon. 2021;7:e06923.
[37] Nokwethemba Sibiya P, Xaba T, Justice Moloto M. Green synthetic approach for starch capped silver nanoparticles and their antibacterial activity, Pure and Applied Chemistry. 2016;88:61–69.
[38] Kumar B, Smita K, Cumbal L, Debut A, Nath Pathak R. Sonochemical synthesis of silver nanoparticles using starch: A Comparison, Bioinorganic Chemistry and Applications. 2014;2014:784268.

[39] Lomelí-Marroquín D, Medina Cruz D, Nieto-Argüello A, Vernet Crua A, Chen J, Torres-Castro A, Webster TJ, Cholula-Díaz JL. Starch-mediated synthesis of mono- and bimetallic silver/gold nanoparticles as antimicrobial and anticancer agents, International Journal of Nanomedicine. 2019;14:2171–2190.

[40] Chinthalapudi N, Vasini Devi Kommaraju V, Kumar Kannan M, Babu Nalluri C, Varanasi S. Composites of cellulose nanofibers and silver nanoparticles for malachite green dye removal from water, Carbohydrate Polymer Technologies and Applications. 2021;2:100098.

[41] Nassaji-Jahromi L, Fazaeli R, Behjatmanesh-Ardakani R, Taghdiri M. Photocatalytic degradation/adsprption of carcinogenic azo dye disperse red 176.1 by nanocage Cu_2O as a dual function catalyst on the visible-light, Journal of the Chilean Chemical Society. 2020;65:5027-5034.

[42] Parvekar P, Palaskar J, Metgud S, Maria R, Dutta S. The minimum inhibitory concentration (MIC) and minimum bactericidal concentration (MBC) of silver nanoparticles against Staphylococcus aureus, Biomaterial Investigations in Dentistry. 2020;7:105-109.

[43] Guy N, Ozacar M. The influence of noble metals on photocatalytic activity of ZnO for Congo red degradation, International journal of hydrogen energy. 2016;41:20100–20112.

[44] Ozcelik Kazancioglu E, Aydin M, Arsu N. Photochemical synthesis of bimetallic gold/silver nanoparticles in polymer matrix with tunable absorption properties: Superior photocatalytic activity for degradation of methylene blue, Materials Chemistry and Physics. 2021;269:124734.